DOI 10.5012/bkcs.2010.31.8.2170

The Interfacial Nature of TiO_2 and ZnO Nanoparticles Modified by Gold Nanoparticles

Yeji Do, Jae-Soo Choi,† Seoq K. Kim, and Youngku Sohn*

Department of Chemistry, Yeungnam University, Gyeongsan, Gyeongbuk 712-749, Korea
†Center for Research Facilities, Chungnam National University, Daejeon 305-764, Korea
**E-mail: youngkusohn@ynu.ac.kr*
Received May 15, 2010, Accepted June 5, 2010

The surfaces of TiO_2 and ZnO nanoparticles have been modified by gold (Au) nanoparticles by a reduction method in solution. Their interfacial electronic structures and optical absorptions have been studied by depth-profiling X-ray photoelectron spectroscopy (XPS) and UV-vis absorption spectroscopy, respectively. Upon Au-modification, UV-vis absorption spectra reveal a broad surface plasmon peak at around 500 nm. For the as-prepared Au-modified TiO_2 and ZnO, the Au $4f_{7/2}$ XPS peaks exhibit at 83.7 and 83.9 eV, respectively. These are due to a charge transfer effect from the metal oxide support to the Au. For TiO_2, the larger binding energy shift from that (84.0 eV) of bulk Au could indicate that Au-modification site of TiO_2 is different from that of ZnO. On the basis of the XPS data with sputtering depth, we conclude that cationic (1+ and 3+) Au species, plausibly $Au(OH)_x$ (x = 1-3), commonly form mainly at the Au-TiO_2 and Au-ZnO interfaces. With Ar^+ ion sputtering, the oxidation state of Ti dramatically changes from 4+ to 3+ and 2+ while that (2+) of Zn shows no discernible change based on the binding energy position and the full-width at half maximum (FWHM).

Key Words: Interfacial electronic structure, X-ray photoelectron spectroscopy, Au-modification, TiO_2, ZnO

Introduction

Metallic nanoparticles supported on transition metal oxides have extensively been studied because the nature of overlayer metal could be modified by the support, and the major role of the overlayer metal could be improved further.[1-5] For an example, Au nanoparticles on oxide support are active for CO oxidation although bulk Au itself is inactive.[1-4] The physical properties (e.g., band gap) and the major role (e.g., catalytic property) of oxide support could also be modified by the overlayer metal. Additionally, surface modification of inorganic nanoparticles by Au has been introduced to prepare for biocompatible inorganic/Au nanoparticles, and thereby the surface is further functionalized by organic molecules.[6,7] Among transition metal oxides, TiO_2 (titanium dioxide) and ZnO (zinc oxide) have widely been studied for various applications including optoelectronic devices, photocatalysts and solar cell devices. In dye-sensitized solar cells (DSSC) and photocatalysts, TiO_2 is one of the most studied materials, and is still explosively under investigation.[8-10] ZnO with a wide direct bad gap of 3.2~3.4 eV has been applied to light emitting diodes and sensors.[11-13]

For a prototype overlayer metal, it is known that Au becomes catalytically active as the size approaches to nanometer-size region. In addition, the activity of Au highly depends on the support material.[1-4] It has been found that Au on TiO_2 support plays a very active catalytic role in CO oxidation at low temperatures, propene epoxidation, and water gas shift reaction ($CO + H_2O \rightarrow CO_2 + H_2$).[14-18] The enhanced catalytic role has been explained by size, shape, and support electronic effects.[19-21] It has been believed that interfacial electronic structures formed between Au and oxide support could play a major role in catalysis.[21,22] It is still not clearly understood that the active catalytic site of Au on oxide support is merely metallic Au and/or ionic Au species.[23] To fully understand the role of metallic nanoparticles on metal oxides, it is very important to study the interfacial electronic structures of Au-metal oxide. In this paper, we have prepared Au nanoparticles on metal oxide nanoparticles by a wet impregnation method in solution. The interface has mainly been studied by depth-profiling XPS.

Experimental Section

Anatase TiO_2 (99.7%, < 25 nm in size) and ZnO (99.7%, < 100 nm in size) nanopowders were purchased from Aldrich, and dispersed in Millipore water (18.1 MΩ-cm resistivity) assisted by an ultrasonicator. In the nanopowder solutions, an appropriate amount of 0.1% hydrogen tetrachloroaurate ($HAuCl_4$, Aldrich) solution was added and boiled while being kept stirred. In the boiling solutions, 0.05 M sodium citrate solution was then added and continued to boil until the color of the solutions was changed. When no further change in color was observed, we stopped boiling and let the solution cool to room temperature. We observed that the originally white TiO_2 and ZnO solutions become violet and pink upon Au-modification, respectively. The change in color indicates that Au nanoparticles become deposited on the metal oxide surfaces. The Au-modified TiO_2 and ZnO in solution were then drop-coated on a Si substrate, and the sample was dried before XPS characterization. UV-vis absorption spectra of the solution samples were taken using a Jasco UV-vis spectrophotometer (V-530). The XPS measurements with Ar^+ ion sputtering depth were performed using a Thermo-VG Scientific MultiLab 2000 with a monochromatic

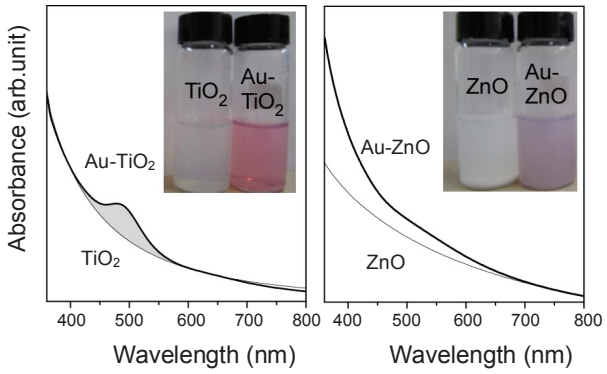

Figure 1. UV-vis absorption spectra of unmodified (thin lines) and Au-modified (thick lines) TiO_2 and ZnO dispersed in water. Digital camera shots clearly show a difference in color before and after Au-modification.

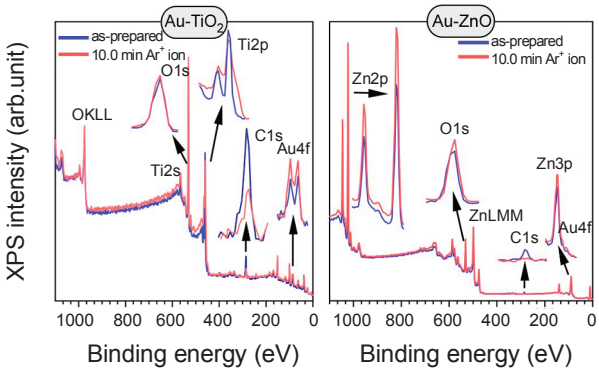

Figure 2. XPS survey spectra of Au-TiO_2 (left) and Au-ZnO (right) before (as-prepared) and after 10.0 min Ar^+ ion sputtering. The C 1s XPS peaks are 5× expanded, but other major peaks are expanded with an arbitrary scale.

Al Kα X-ray source (1486.6 eV), a pass energy of 20.0 eV, and a hemispherical energy analyzer. Because no critical final state surface charging effect was observed during the XPS measurements, no binding energy correction was performed for the obtained XPS spectra.

Results and Discussion

Figure 1 shows the UV-vis spectra of TiO_2 (left) and ZnO (right) nanoparticle solutions before and after a surface modification by Au nanoparticles. Compared to the spectra of un-modified nanoparticles, those of the modified particles clearly show an enhanced absorption intensity at around 400 ~ 600 nm. In addition, the Au-modified TiO_2 and ZnO solutions are pink and violet, respectively, as seen from the photos in Figure 1. It is known that the surface plasmon peak of Au nanoparticles depends on size, concentration and aggregation.[24] On the basis of the peak position for Au-TiO_2 and the literature information,[24] we deduce that the size of Au nanoparticles is not larger than 5 nm. For Au-ZnO, the Au particle size is likely bigger (but less dense) than that for Au-TiO_2 with a broader size distribution. For ZnO, the larger Au particle size could be expected because the size of ZnO particle is 4 × of that of TiO_2, and thus the surface area for Au nanoparticle growth is larger for ZnO.

The samples were further characterized by depth profiling

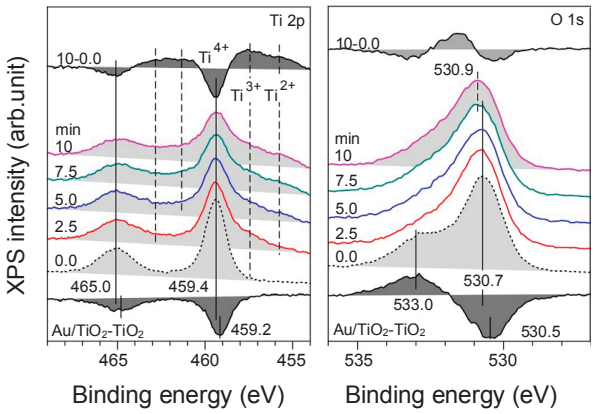

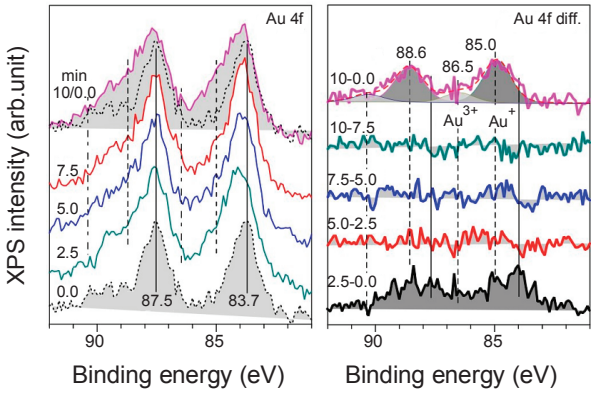

Figure 3. Ti 2p, O 1s, Au 4f, and Au 4f difference XPS spectra of Au-TiO_2 with Ar^+ ion sputtering time. 10/0.0: the spectra for 10 min and 0.0 min are displayed with the same baseline. 10-0.0 difference spectrum: subtraction of the spectrum of 0.0 min from that of 10 min. Au/TiO_2-TiO_2 difference spectrum: subtraction of the spectrum of as-prepared bare TiO_2 from that of as-prepared Au-TiO_2.

XPS to clarify changes in chemical state and electronic structure with sputtering depth. Figure 2 shows the XPS survey spectra before and after (10 min Ar^+ ion sputtering) depth profiling for Au-modified TiO_2 and ZnO, respectively. The main XPS peaks are expanded to illustrate a noteworthy change in peak. The C 1s XPS peaks show a dramatic decrease upon sputtering with no critical change in peak position, attributable to contaminated carbon species. Interestingly, before sputtering the C 1s XPS peak for Au-TiO_2 is 10× stronger than that for Au-ZnO. After sputtering, the C 1s XPS peak for Au-ZnO is almost completely disappeared while that for Au-TiO_2 exhibits a considerable intensity. From the results, we could deduce that the surface area of TiO_2 is larger than that of ZnO. In addition, the Au-TiO_2 may be chemically more active than Au-ZnO, and consequently contain more contaminated carbon species on the surface. As mentioned in the experimental section, we used TiO_2 smaller in size than ZnO. For Au-TiO_2, the Ti 2p XPS peaks are significantly broadened, indicating a dramatic change in chemical state. The intensity of Au 4f XPS peak is enhanced in the higher binding energy side. For Au- ZnO, the Zn 2p XPS peaks are considerably enhanced with no significant change in peak position. Further details will be described below with high-resolution XPS spectra displayed in Figure 3 and 4 for Au-TiO_2 and Au-ZnO, respectively.

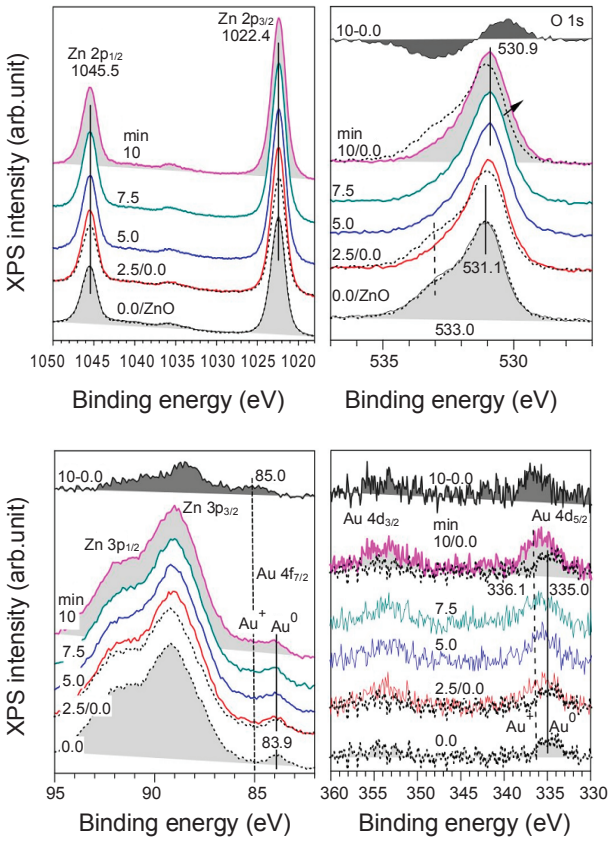

Figure 4. Zn 2p, O 1s, Zn 3p, Au 4f, and Au 4d spectra of Au-ZnO with Ar^+ ion sputtering time. All the dotted lines are the spectra of the as-prepared (0.0 min) sample. 0.0/ZnO: the spectra of as-prepared (0.0 min) Au-ZnO and bare ZnO are displayed with the same baseline. 10/0.0: the spectra for 10 min and 0.0 min are displayed with the same baseline. 10-0.0 difference spectrum: subtraction of the spectrum of 0.0 min from that of 10 min.

In Figure 3, for Au-TiO_2 before sputtering, the Ti $2p_{3/2}$ (Ti $2p_{1/2}$) XPS peak is located at 459.4 eV (465.0 eV), with a spin-orbit splitting of 5.6 eV. This is in good agreement with literature values for bare TiO_2 (oxidation state of 4+ for Ti)[25-27] To clarify a change in Ti 2p XPS peak upon Au-modification, we subtracted the Ti 2p XPS of Au-TiO_2 from that of bare TiO_2. The difference Ti 2p XPS is displayed below the Ti 2p XPS spectrum of the as-prepared (0.0 min) Au-TiO_2. The total intensity of Ti 2p peak is decreased by 35% upon Au-modification. The negative Ti $2p_{3/2}$ peak position is located at 459.2 eV, 0.2 eV lower than 459.4 eV. The decrease in lower BE side emission is possibly due to a charge transfer effect by the overlayer Au nanoparticles and adsorbed OH (or H_2O). The O 1s XPS peak also slightly shifts to a higher BE side upon Au-modification, plausibly due to the same reasons. The O 1s XPS peak exhibits two peaks at 530.7 and 533.0 eV, with an intensity ratio of 2.7/1 ($I_{530.7}/I_{533.0}$). The major peak at 530.7 eV is due to oxygen of TiO_2, and the minor shoulder peak is attributed to adsorbed hydroxyl groups, defective oxides and/or adsorbed water.[25-27] A difference O 1s XPS peak between the spectra of as-prepared Au-TiO_2 and bare TiO_2 is also displayed. Upon Au-modification, the major O 1s peak is decreased by 28% while the minor peak at 533.0 eV is enhanced by 72 %. The total O 1s XPS area is decreased by merely 13%, smaller than 35% decrease in the Ti 2p peak. Solely based on the larger decrease in Ti 2p XPS intensity upon Au-modification, it could be deduced that OH (or H_2O) group is mainly adsorbed on Ti site by forming Ti-O-H bonds. Our XPS result is consistent with the OH (or H_2O) adsorption model based on IR spectroscopic result reported by Bezrodna *et al*.[28]

To calculate the relative elemental composition of Ti *versus* O, the peaks of Ti 2p and O 1s XPS are integrated, and the areas are divided by their corresponding sensitivity factors (Ti 2p = 1.8 and O 1s = 0.66).[29] Then, the Ti/O ratio is calculated to be 1/3.6; oxygen is richer, compared to 1/2 of TiO_2. This is mainly due to adsorbed by OH (or H_2O) species, and Ti is mainly covered by the species, as discussed above. For Au 4f XPS, the Au $4f_{7/2}$ (Au $4f_{5/2}$) XPS peak is located at 83.7 (87.5) eV, with a spin-orbit splitting of 3.8 eV. The BE position is lower than that (84.0 eV) of bulk metallic gold. This is due to either a charge transfer effect or an initial state quantum size (or electronic) effect. This will be further discussed later. Using the XPS areas and their corresponding sensitivity factors the Au/Ti ratio is calculated to be 1/30. Assuming that the radius of a spherical TiO_2 particle is < 12 nm, and using the volume ($4/3\ \pi r^3$) of a sphere particle, we roughly calculated the radius of an Au particle to be < 3.8 nm, corresponding to < 7.4 nm in size. Because an inelastic electron mean free path (IMFP) as a factor is not considered in this rough calculation, and the IMFP is likely smaller than the size of TiO_2 particle[25,29] the real size must be smaller than the calculated value. As discussed above, the Au size is not larger than 5 nm expected from the UV-vis absorption spectrum.

High-resolution XPS spectra were recorded with increasing Ar^+ ion sputtering time. Upon 2.5 min sputtering, the Ti 2p XPS shows a dramatic change. The major peak at 459.4 eV is reduced by 22%, with no discernible change in peak position. However, the photoelectron emission in the lower BE side is newly appeared. We attribute the lower BE side emission to reduced Ti states (Ti^{n+}, n < 4) formed during Ar^+ ion sputtering.[30-32] The total Ti 2p XPS is enhanced by 17% after an initial 2.5 min sputtering, due to removal of adsorbed overlayer species, such as OH (or H_2O) groups. With further increasing sputtering, the Ti $2p_{3/2}$ peak (Ti^{4+}) at 459.4 eV is gradually decreased while the Ti $2p_{3/2}$ peak at lower BE sides is constantly increased. A difference spectrum (10.0 - 0.0) between the as-prepared sample and the 10.0 min-sputtered sample shows negative and broader positive peaks, corresponding to Ti^{4+} and Ti^{n+} (n < 4), respectively. For the O 1s XPS upon sputtering, the peak at 533.0 eV is reduced while the O 1s peak of TiO_2 crystal lattice at 530.7 eV is enhanced, due to removal of adsorbed OH (or H_2O) groups. With increasing the sputtering time, the O1s XPS peak gradually shifts to a higher BE position by + 0.2 eV. The enhanced emission in the higher BE could be due to sputtering-induced defective oxides.[25-27] For bare TiO_2 with sputtering we have also observed that the major O 1s XPS peak gradually shifts to a higher BE position.

For the Au 4f XPS with increasing sputtering time, the peak broadens and shifts to a higher BE position. The difference spectrum between the as-deposited (0.0 min) and the 10 min-sputtered samples could be fitted with two $4f_{7/2}$ XPS peaks at 85.0 and 86.5 eV. The peaks at 85.0 and 86.5 eV are plausibly assign-

ed to Au^+ and Au^{3+} states, respectively. The XPS intensity ratio ($I_{85.0}$ /$I_{86.5}$) of the two peaks is estimated to be 3.9/1, and the (Au^{3+} + Au^+)/Au^0 ratio (cationic *vs*. metallic species) for the 10 min-sputtered sample is estimated to be 0.63/1. For Au-TiO_2 prepared by a deposition-precipitation (DP) method, Fu *et al*. observed Au^+ and Au^{3+} (AuO^-, AuO_2^- and $AuOH^-$) species by time-of-flight secondary ion mass spectroscopy (TOF-SIMS),[33] consistent with our XPS result showing the same oxidation states. However, they observed only metallic Au by XPS without any indication of ionic Au species. For the as-prepared un-sputtered sample, our XPS data show only metallic Au. Mrowetz *et al*. also observed only a metallic Au $4f_{7/2}$ peak at 83.6 eV.[34] On the other hand, for an as-prepared sample Casaletto *et al*. found two $4f_{7/2}$ XPS peaks at 84.4 and 85.6 eV (obtained after curve-fitting), assigned to Au^0 (67%) and Au^{3+} (33%), respectively.[35] Yang *et al*. found an Au $4f_{7/2}$ (Au $4f_{5/2}$) peak at 85.8 eV (89.1 eV), assigned to Au^{3+} species.[36] The inconsistent XPS results could be explained as follows: the cationic Au species form mainly at the interface. If the Au particle size is big enough, the photo-emitted signal from the interface could not travel to the surface without energy loss because of a short inelastic electron mean free path, while the size is small enough the photoelectrons both from the surface (Au^0) and the interface (Au^+ and Au^{3+}) could reach the surface. For Au nanoparticles on TiO_2(110) studied by scanning tunneling microscopy (STM) and density functional theory (DFT) calculation, Matthey *et al*. made a conclusion that cationic Au species are generally occurred at the interface.[37]

The higher Au 4f XPS BE could also be due to a final state quantum size effect.[38-40] Because the size of Au particles could be decreased to a quantum size by sputtering, a quantum size effect should be discussed. At lower coverages of Au on TiO_2 (110) surface prepared in an UHV condition, it has been observed that the $4f_{7/2}$ XPS peak show ~ 0.5 eV higher BE than that of metallic Au, attributed to a final state screening effect.[39,40] Jiang *et al.* reported a XPS evidence that on reduced TiO_2 (110) surface charge transfer from the oxide support to Au also play a role in the XPS BE.[40] However, for the samples prepared in solution, the $4f_{7/2}$ XPS BE exhibits at much higher position than the BE induced by final-state quantum size or charge transfer effects.

For the un-sputtered sample as mentioned above, the $4f_{7/2}$ XPS peak at 83.7 eV is in good agreement with the result reported by Radnik *et al*.[41] They observed lower $4f_{7/2}$ XPS BE than that of metallic Au for Au supported on TiO_2 nanoparticles, prepared by chemical vapor deposition and deposition-precipitation methods. This could be explained by a charge transfer effect from the support to Au. It has been believed that Au is attracted more strongly to oxygen vacancy sites than to Ti or bridging oxygen sites.[42] In this case, the electron from the vacancy will transfer to adlayer Au. This indicates that a stronger bonding between Au and TiO_2 support is expected for defect-rich TiO_2 support.

For the as-prepared ZnO shown in Figure 4, the Zn $2p_{3/2}$ (Zn $2p_{1/2}$) XPS peak is located at 1022.4 (1045.5) eV, with a spin-orbit splitting of 23.1 eV. This is attributed to Zn(II) of ZnO crystal lattice. For the O 1s XPS of ZnO, the peak consists of at least two peaks at 531.1 and 533.0 eV. The shoulder peak at 533.0 eV could be assigned to adsorbed OH (H_2O) species on the surface,[13] as mentioned above. The Au $4f_{7/2}$ XPS peak is clearly seen at 83.9 eV although the Au $4f_{5/2}$ XPS peak is buried in the strong Zn $3p_{3/2}$ XPS peak. A weak Au $4d_{5/2}$ XPS peak is seen at 335.0 eV, assigned to metallic Au.[25,26] Compared to the Au $4f_{7/2}$ XPS BE (83.7 eV) for Au-TiO_2, the BE for Au-ZnO is higher and is more close to that (84.0 eV) for bulk metallic Au, in good agreement with the literature.[41] This indicates that the adsorption site (e.g., vacant Zn interstitial surface sites exhibiting less charge transfer to Au)[43] of Au on ZnO is different from that (e.g., oxygen vacancy sites)[42] of Au on TiO_2. Although it has not clearly been understood why nanosize Au on oxide support is chemically active, the larger Au 4f BE shift for Au-TiO_2 than that for Au-ZnO could be related with the fact that Au is more active on TiO_2 support than on ZnO.[1-3] Using the Zn 2p and the Au 4f XPS areas, and their corresponding sensitivity factors the Au/Zn composition ratio is calculated to be 1/80.

Upon sputtering the sample for 2.5 min, the Zn 2p XPS intensity is enhanced by 26%. This is mainly due to removal of adsorbed OH (H_2O) species.[44] The O 1s XPS peak at 533.0 eV is reduced as expected while the major O 1s peak at 531.1 eV shifts to a lower BE position by 0.2 eV. The difference spectrum between 10 min (solid line) and 0.0 min (broken line) show a broad negative peak at 533.0 eV and a positive peak. The two spectra are displayed with the same baseline in Figure 4 for a direct comparison. With further increasing sputtering time, although the Zn 2p becomes slightly enhanced the peak position and the FWHM stay nearly constant, indicating no critical change in chemical environments. For the Au $4f_{7/2}$ XPS, with increasing sputtering time the photoemission signal at around 85.0 eV becomes enhanced. The difference spectrum between 10 min (solid line) and 0.0 min (broken line) clearly show a broad positive peak at ~85.0 eV. This could be due to Au(I) species, as discussed above for Au-TiO_2. The Au $4d_{5/2}$ XPS peak becomes broader and stronger, mainly due to an increase in photoemission signal at ~336.1 eV, assigned to Au(I). The difference spectrum (10min - 0.0min) clearly shows a peak at 336.1 eV. The Au 5d spectra of 10 min (solid line) and 0.0 min (broken line) are compared with the same baseline. Because the Au 4f peak is buried in the Zn 3p, and the Au 5d spectra is much weaker we could not clearly deduce whether Au(III) species are present or not for Au-ZnO. However, on the basis of the result of Au-TiO_2, we assume Au(III) species are also probably present at the Au-ZnO interface. Phala *et al*. demonstrated by a theoretical calculation that Au(I), Au(II) and Au(III) are stable as substitutional species of vacant Zn(II).[42] For Au-ZnO samples prepared in solution, $Au(OH)_x$ (x = 1 - 3) complexes are plausibly formed as cationic Au species.[42]

Summary

TiO_2 and ZnO nanoparticle surfaces have been modified by Au nanoparticles by a deposition-precipitation method in solution, and investigated by depth-profiling XPS and UV-vis absorption spectroscopy. On the basis of Au 4f XPS with sputtering time, we conclude that cationic (1+ and 3+) Au species are commonly formed, mainly at the interface of Au and the oxide nanoparticles. With the Au 4f (Au^+ and Au^{3+}) and O 1s XPS data (e.g., OH) in conjunction with a literature report,[42] we as-

sume that the cationic Au species are plausibly due to $Au(OH)_x$ (x=1 - 3). For the unsputtered as-prepared samples, the only metallic Au 4f XPS peaks observed at 83.7 and 83.9 eV for TiO_2 and ZnO, respectively. It appears that charge transfer from the adsorption sites on TiO_2 to Au nanoparticles is more prominent than from those on ZnO to Au nanoparticles. A critical difference between TiO_2 and ZnO with Ar^+ ion sputtering is that the oxidation state (4+) of Ti for TiO_2 is dramatically changed to lower oxidation states (3+ and 2+) while that (2+) of Zn for ZnO shows no noticeable change. Our XPS results much clearly reveal the interfacial electronic structures of two different metal oxides TiO_2 and ZnO modified by Au nanoparticles.

Acknowledgments. This research was supported by the Yeungnam University research grants in 2008.

References

1. Haruta, M. *Catal. Today* **1997**, *36*, 153.
2. Haruta, M. *Cattech* **2002**, *6*, 102
3. Meyer, R.; Lemire, C.; Shaikhutdinov, Sh. K.; Freund, H.-J. *Gold Bull*. **2004**, *37*, 72.
4. Pirkanniemi, K.; Sillanpää, M. *Chemosphere* **2002**, *48*, 1047.
5. Kudo, A.; Miseki, Y. *Chem. Soc. Rev*. **2009**, *38*, 253.
6. Liu, Y.; Zhong, M.; Shan, G.; Li, Y.; Huang, B.; Yang, G. *J. Phys. Chem. B* **2008**, *112*, 6484.
7. Wang, X.; Kong, X.; Yu, Y.; Zhang, H. *J. Phys. Chem. C* **2007**, *111*, 3836.
8. Linsebigler, A. L.; Lu, G.; Yates, J. T., Jr. *Chem. Rev*. **1995**, *95*, 735.
9. Ni, M.; Leung, M. K. H.; Leung, D. Y. C.; Sumathy, K. *Renew. Sust. Energy Rev*. **2007**, *11*, 401.
10. Wold, A. *Chem. Mater.* **1993**, *5*, 280.
11. Özgür, Ü.; Alivov, Ya. I.; Liu, C.; Teke, A.; Reshchikov, M. A.; Doan, S.; Avrutin, V.; Cho, S. -J.; Morkoç, H. *J. Appl. Phys.* **2005**, *98*, 041301.
12. Klingshirn, C. *Phys. Stat. Sol. (b)* **2007**, *244*, 3027.
13. Woll, C. *Prog. Surf. Sci*. **2007**, *82*, 55.
14. Valden, M.; Paka, S.; Lai, X.; Goodman, D. W. *Catal. Lett.* **1998**, *56*, 7.
15. Chen, M.; Goodman, D. W. *Chem. Soc. Rev*. **2008**, *37*, 1860.
16. Hashmi, A. S. K.; Hutchings, G. J. *Angew. Chem., Int. Ed.* **2006**, *45*, 7896.
17. Andreeva, D. *Gold Bull.* **2002**, *35/3*, 83.
18. Bond, G. C.; Sermon, P. A.; Webb, G.; Buchanan, D. A.; Wells, P. B. *J. Chem. Soc., Chem. Commun*. **1973**, 444.
19. Chen, M. S.; Goodman, D. W. *Science* **2004**, *306*, 252.
20. Parker, S. C.; Campbell, C. T. *Top. Catal*. **2007**, *44*, 3.
21. Cosandey, F.; Madey, T. E. *Surf. Rev. Lett*. **2001**, *8*, 73.
22. Chusuei, C. C.; Lai, X.; Luo, K.; Goodman, D. W. *Topics Catal.* **2001**, *14*, 71.
23. Raphulu, M. C.; McPherson, J.; van der Lingen, E.; Anderson, J. A.; Scurrell, M. S. *Gold Bull*. **2010**, *43*, 21.
24. Haiss, W.; Thanh, N. T. K.; Aveyard, J.; Fernig, D. G. *Anal. Chem.* **2007**, *79*, 4215.
25. Moulder, J. F.; Stickle, W. F.; Sobol, P. E.; Bomben, K. D. *Handbook of X-ray Photoelectron Spectroscopy*, 2nd ed.; Chastain, J., Ed.; Perkin-Elmer Corp.: Eden-Prairie, MN, 1992.
26. NIST, *X-ray Photoelectron Spectroscopy Database*, NIST Standard Reference Database 20, Version 3.5 (Web version: http://srdata.nist.gov/xps/).
27. Liu, G.; Jaegermann, W.; He, J.; Sundstrom, V.; Sun, L. *J. Phys. Chem. B* **2002**, *106*, 5814.
28. Bezrodna, T.; Puchkovska, G.; Shymanovskaa, V.; Baran, J.; Ratajczak, H. *J. Mol. Struc*. **2004**, *700*, 175.
29. Briggs, D.; Seah, M. P. *Practical Surface Analysis*, 2nd ed.; Vol. 1, Wiley and Sons: 1990.
30. Fu, Q.; Wagner, T.; Olliges, S.; Carstanjen, H.-D. *J. Phys. Chem. B* **2005**, *109*, 944.
31. Takeuchi, M.; Onozaki, Y.; Matsumura, H.; Uchida, H.; Kuji, T. *Nucl. Instrum. Meth. B* **2003**, *206*, 259.
32. Henrich, V. E.; Dresselhaus, G.; Zeiger, H. J. *Phys. Rev. Lett*. **1976**, *36*, 1335.
33. Fu, L.; Wu, N. Q.; Yang, J. H.; Qu, F.; Johnson, D. L.; Kung, M. C.; Kung, H. H.; Dravid, V. P. *J Phys. Chem. B* **2005**, *109*, 3704.
34. Mrowetz, M.; Villa, A.; Prati, L.; Selli, E. *Gold Bull*. **2007**, *40*(2), 154.
35. Casaletto, M. P.; Longo, A.; Martorana, A.; Prestianni, A.; Venezia, A. M. *Surf. Interface Anal.* **2006**, *38*, 215.
36. Yang, J. H.; Henao, J. D.; Raphulu, M. C.; Wang, Y. M.; Caputo, T.; Groszek, A. J.; Kung, M. C.; Scurrell, M. S.; Miller, J. T.; Kung, H. H. *J. Phys. Chem. B* **2005**, *109*, 10319.
37. Matthey, D.; Wang, J. E.; Wendt, S.; Matthiesen, J.; Schaub, R.; Lægsdaard, E.; Hammer, B.; Besenbacher, F. *Science* **2007**, *315*, 1692.
38. Zhang, P.; Sham, T. K. *Phys. Rev. Lett.* **2003**, *90*, 245502.
39. Zhang, L.; Persaud, R.; Madey, T. E. *Phys. Rev B* **1997**, *56*, 10549.
40. Jiang, Z.; Zhang, W.; Jin, L.; Yang, X.; Xu, F.; Zhu, J.; Huang, W. *J. Phys. Chem. C* **2007**, *111*, 12434.
41. Radnik, J.; Mohr, C.; Claus, P. *Phys. Chem. Chem. Phys*. **2003**, *5*, 172.
42. Wahlstrom, E.; Lopez, N.; Schaub, R.; Thostrup, P.; Ronnau, A.; Africh, C.; Laegsgaard, E.; Norskov, J. K.; Besenbacher, F. *Phys. Rev. Lett*. **2003**, *90*, 026101.
43. Phala, N. S.; Klatta, G.; van Steen, E.; French, S. A.; Sokolb, A. A.; Catlow, C. R. A. *Phys. Chem. Chem. Phys*. **2005**, *7*, 2440.
44. Mosbacker, H. L.; Strzhmechny, Y. M.; White, B. D.; Smith, P. E.; Look, D. C.; Reynolds, D. C.; Litton, C. W.; Brillson, L. J. *Appl. Phys. Lett*. **2005**, *87*, 012102.